Journal of Alloys and Compounds 657 (2016) 770–776

Contents lists available at ScienceDirect

Journal of Alloys and Compounds

journal homepage: http://www.elsevier.com/locate/jalcom

Experimental investigation of liquidus and phase stability in the $BaO-SiO_2$ binary system

Rui Zhang*, Pekka Taskinen

Aalto University, School of Chemical Technology, Metallurgical Thermodynamics and Modelling Research Group, Espoo, Finland

ARTICLE INFO

Article history:
Received 31 July 2015
Received in revised form
5 October 2015
Accepted 19 October 2015
Available online 21 October 2015

Keywords:
Slag
SEM/EDS
EPMA
XRD
Calculated phase diagram
MTOX oxide database

ABSTRACT

The liquidus in the SiO_2-rich corner was experimentally constructed at temperatures from 1400 °C to 1640 °C. The phase compositions of the liquidus studied were obtained by analyzing the quenched samples employing Scanning Electron Microscopy/Energy Dispersive X-ray Spectroscopy (SEM/EDS) and Electron Probe Micro-Analyzer (EPMA). The phase relationships of the stoichiometric compounds at 1200 °C and 1250 °C were determined by X-ray powder diffraction (XRD). Phase diagram of the $BaO-SiO_2$ binary system was calculated based on the MTOX oxide database. The present experimental data were compared with the calculated phase diagram and showed a good agreement.

1. Introduction

The $BaO-SiO_2$ binary system is of significant importance in glass, ceramic technology and extractive metallurgy. The addition of $BaO-SiO_2-B_2O_3$ glass into $BaTiO_3$-based ceramics helps to decrease the sintering temperature and refine the microstructure [1–4], while the complex reaction of glass formation restricts the improvement of density of energy storage of the $BaTiO_3$-based ceramics. Knowledge of the thermodynamic and experimental information of the liquid phase is critical to achieve optimal compositions and processes of glasses exhibiting optimized photoluminescence effect. Meanwhile, the properties of alkaline slags with respect to the behaviors of impurities have been known for a long time, but they are not fully understood because of lack of thermodynamic data on these systems [5]. However, interest in these slags is rapidly increasing because of their ability to eliminate hazardous impurities and to decrease the loss of valuable metals into slags [6].

Barium oxide is considered as a more basic oxide than calcium oxide as the major basic constituent of ironmaking and steelmaking slags [7–9]. The $BaO-SiO_2$ system is one part of BaO-containing slags ($BaO-MgO-CaO-Al_2O_3-SiO_2$) for extractive metallurgy in refining. Good description of phase stabilities and thermodynamic properties of $BaO-SiO_2$ system is essential for the completion of this binary phase diagram and can serve as the foundation for the extrapolation of BaO-bearing multi-components systems. In addition, it can contribute to complete the complex oxide database, for example, MTOX database employed in smelting and refining [10]. Due to the high temperature (above 1400 °C) for the experiments of the $BaO-SiO_2$ system, disagreement exists at certain compositional regions in the available literature data. Consequently, extra phase relation descriptions are required to acquire a better understanding of this system.

The present work aims to investigate (1) the liquidus in the SiO_2-rich corner of the $BaO-SiO_2$ binary system from 1350 °C to 1640 °C; (2) the solid state phase equilibria of the stoichiometric compounds at 1200 °C and 1250 °C and (3) to perform thermodynamic calculation of this system on the basis of MTOX oxide database [10]. For the sake of simplicity, symbols B and S were used as abbreviations of BaO and SiO_2, thus B_3S, B_2S, BS, B_2S_3, B_5S_8, B_3S_5 and BS_2 stand for Ba_3SiO_5, Ba_2SiO_4, $BaSiO_3$, $Ba_2Si_3O_8$, $Ba_5Si_8O_{21}$, $Ba_3Si_5O_{13}$ and $BaSi_2O_5$ if not stated otherwise.

* Corresponding author. P.O Box 16200, FI-00076 Aalto, Finland.
E-mail address: rui.2.zhang@aalto.fi (R. Zhang).

http://dx.doi.org/10.1016/j.jallcom.2015.10.165
0925-8388/

2. Literature review

The $BaO–SiO_2$ system was experimentally investigated and thermodynamically calculated by several authors [11–21]. The liquidus in the SiO_2-rich region was firstly measured by Greig [11] using the quenching technique. It was observed that the liquidus rises steeply and then follows a flat curve from 85 to 97 mol% SiO_2 at around 1680 °C. Greig [11] explained that with the melting temperature of cristobalite of 1710 °C [12], it is impossible to draw a liquidus line of normal shape which can fit these results. Therefore, the melting point of cristobalite was re-measured again by Greig [11] based on a serious of quenches and fixed at 1713 ± 5 °C. By means of quenching method in conjunction with microscopic examination, Kracek [13] constructed the cristobalite liquidus in the alkali oxide-silica system (Mg, Ca, Sr, Ba, Li, Na, K, Rb and Cs) and indicated no existence of miscibility gap from BaO to Cs_2O. On the other hand, a characteristic type of reverse S type cristobalite melting curve was presented in the system with BaO, Li_2O and Na_2O. This S type liquidus in barium oxide-silica system was also observed by Ol'Shanskij [14], focusing on the temperatures ranging from 1600 °C to 2200 °C.

Eskola [15] measured the $BaO–SiO_2$ system employing the quenching method. Ba_2SiO_4, $BaSiO_3$, $Ba_2Si_3O_8$ and $BaSi_2O_5$ were reported and a complete solid solution exists between dibarium trisilicate and barium disilicate. Later, Levin et al. [16] constructed a phase equilibrium diagram for the system $BaO–B_2O_3–SiO_2$ by the quenching method. The solid solution region was observed between $Ba_2Si_3O_8$ and $BaSi_2O_5$ extending into the interior of the diagram. Then Roth et al. [17] provided a revised phase diagram for the subsystem $Ba_2Si_3O_8–BaSi_2O_5$ that, on the contrary, a complete solid solution series was not verified. According to the data acquired by XRD, two new compounds were identified so that $Ba_3Si_5O_{13}$ melts incongruently at 1423 °C forming $Ba_5Si_8O_{21}$ and liquid, and $Ba_5Si_8O_{21}$ melts congruently at 1446 °C. It was mentioned by Roth et al. [17] that by comparing the X-ray diffraction patterns of $Ba_2Si_3O_8$, $Ba_5Si_8O_{21}$ and $Ba_3Si_5O_{13}$ with decreasing BaO content, instead of a continuous shift in *d* (the height of the strongest peak) values, as the characteristic feature for solid solutions, two phases of constant *d* values always appeared. This conclusion is in agreement with the work by Douglass [18]. All the key experiments discussed above are listed in Table 1.

By means of CALPHAD (CALculation of PHAse Diagram) technique, Shukla [19], Romero [20] and Boulay [21] performed the thermodynamic assessment of the $BaO–SiO_2$ system. The calculated results agree with the experimental measurements by Greig [11] and Roth et al. [17]. The major discrepancy concentrates on the shape of the liquidus at the SiO_2-rich corner which belongs to the focus of the present work.

3. Experiments

3.1. Sample preparation

$BaCO_3$ is widely used as the starting material to acquire BaO. The initial mixtures were prepared from reagent $BaCO_3$ (99.95 wt%, Alfa Aesar, Germany) and SiO_2 (99.99 wt%, Umicore, Belgium) powders. They were dried at 150 °C for 24 h and then mixed with the molar ratio (B:S = 1:9) and ground in an agate mortar, and finally pelletized to the diameter of 5 mm and thickness of 4 mm in a pressing tool. The mass of the pellets is less than 0.2 g. Small bulk of the samples facilitated a good quenching. Platinum wire (99.99 wt %, Johnson-Matthey Noble Metals, England) and commercial SiO_2 crucibles (>99.98 wt%, OM Lasilaite Oy, Finland) were used for suspending and holding the samples throughout the experiment. Since platinum is inert under the experimental condition in the present work and SiO_2 belongs the desired binary system, purity of the system can be preserved.

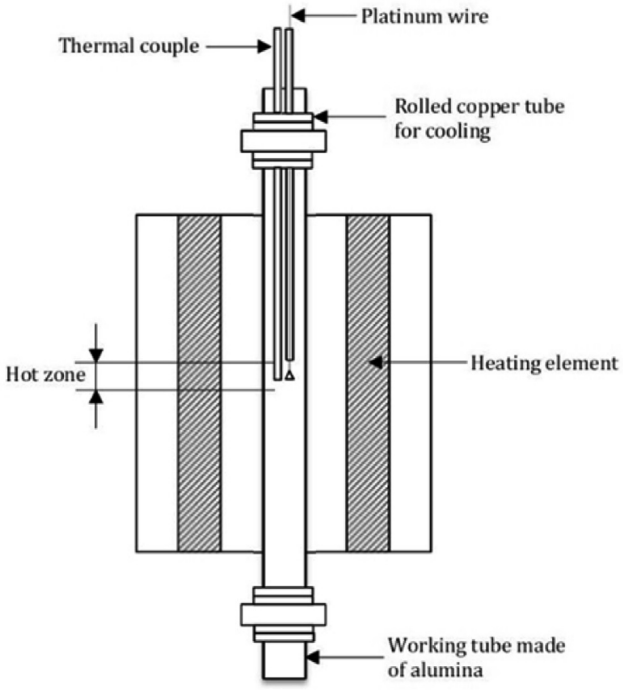

Fig. 1. Schematic picture of the furnace arrangement for equilibration experiment (a).

3.2. Experimental apparatus and procedure

In order to measure the liquidus in SiO_2-rich region and solid state phase equilibria of the stoichiometric compounds, two batches of experiments were conducted.

For the first batch (a), equilibration was accomplished in the furnace (Nabertherm RHTV series vertical tube furnace, Germany) with a vertical Al_2O_3 work tube inside (Fig. 1). Before the experiments, hot zone of the furnace was determined by establishing thermal profile at 900 °C, 1200 °C and 1500 °C. A calibrated S-type thermocouple (Johnson-Matthey Noble Metals, Royston, Herts, UK)

Table 1
Summary of the key experimental data in the literature.

Phase equilibria data	Technique	Ref.
Liquidus of SiO_2-rich region from 1489 °C to 1690 °C	Quenching	[11]
Liquidus of cristobalite for alkali silicate mixtures	Quenching	[13]
Liquidus of SiO_2-rich region from 1600 °C to 1800 °C	Quenching	[14]
Liquidus of tridymite, liquidus of solid solutions $B_2S–B_2S_3$, melting temperature of BS_2 and B_2S_3	Quenching	[15]
Solid solution region between BS_2 and B_2S_3	Quenching and XRD	[16]
Phase diagram for $B_2S–B_2S_3$ subsystem with both end members as stoichiometric compounds, confirmation of B_3S_5 and B_5S_8	Polarizing microscope, quenching and XRD	[17]

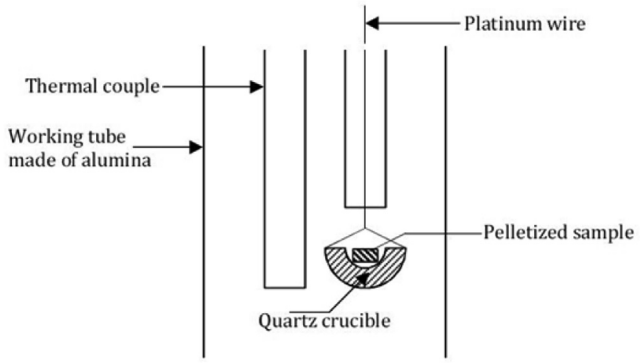

Fig. 2. Schematic picture of the sample and sample holder arrangement.

was connected to a Keithley 2010 multi-meter (Cleveland, OH, USA), and a cold junction compensation was connected to a Keithley 2000 multi-meter (Cleveland, OH, USA) to measure the ambient temperature with a Pt100 sensor (Platinum Resistance Thermometer, SKS Group, Finland). The temperature data throughout the experiments were collected using a NI LabVIEW temperature logging program. The overall accuracy of the measurements was estimated as ±2 °C. Careful consideration was given to the equilibration time. Time series of 4 h, 8 h, 12 h and 24 h was tested to verify the suitable equilibration time. It was found that the achievement of equilibria at and above 1400 °C was within 8 h and longer diffusion time, 24 h, was required at 1350 °C. The attainment of equilibrium was confirmed by two means: 1) for the quenched samples equilibrated at different hours, checking the phases via backscattered electron (BSE) graphs that co-existence of molten phase and crystals at 1400 °C–1640 °C and solid–solid phases at 1350 °C were found; 2) The chemical analysis using Scanning Electron Microscopy/Energy Dispersive X-ray Spectroscopy (SEM/EDS) to check the consistency of compositions of different phases that the results were consistent.

The pelletized sample was placed in a quartz crucible and suspended using a platinum wire from the bottom of the work tube to the hot zone (Fig. 2). The top and bottom of the work tube are open to the atmosphere. Then the sample was held at target temperature to complete the equilibration. After the equilibration was obtained at specific temperature and time, a bottle of a mixture of ice and water was placed under the bottom of the work tube, and then quartz crucible along with the sample was rapidly dropped and quenched by cutting the platinum wire. The quenched sample was dried and mounted in an epoxy resin. To acquire the cross section of the mounted sample, the solidified epoxy resin was ground and polished without introducing water and lubricant. Then the polished specimen was carbon coated using a Leica EM SCD050 Coater (Leica Mikrosysteme GmbH, Wien, Austria) and analyzed by Scanning Electron Microscopy (SEM, A LEO 1450, Carl Zeiss Microscopy GmbH, Jena, Germany) with Energy Dispersive X-ray Spectroscopy (EDS, Link Inca X-sight 7366, Oxford Instruments plc, Abingdon, Oxfordshire, UK) to achieve the microstructures and phase compositions. The accelerating voltage was 15 kV and employed standards were Barite for Ba and Quartz for Si. To guarantee the accuracy of chemical analysis, Electron Probe X-ray Micro-Analyzer (EPMA, CAMECA SX 100, Cameca SAS, France) equipped with five wavelength dispersive spectrometers at Geological Survey of Finland (GTK) was employed. The analyses were performed on every sample at different locations of the phases with total 10 points. The accelerating voltage was 15 kV and beam current was 6 nA. The analyzed lines and standards used were O Ka (hematite), Ba La (barite) and Si Ka (quartz).

For another batch of experiments (b) to investigate phase equilibria of stoichiometric compounds, in order to avoid the formation of barium peroxide at low temperatures, the equilibration was conducted in the protection of argon (99%) and hydrogen (1%). A filter was employed to remove moisture in the gas before flushing into the furnace. A horizontal tube furnace (Heraeus, ROS 4/50, Germany) was employed for the equilibration experiments (Fig. 3). The same method mentioned for experiment batch (a) was adopted to determine the hot zone of this furnace. Five samples with varying compositions were seated on the net made of platinum wires (to avoid contact with alumina) and then put in an alumina crucible boat. The crucible boat was placed at the hot zone of the furnace with flushing gas of Ar (99%) and H_2 (1%). The quenching was conducted by using a hook to pull the boat out of the furnace and placing into the icy water. In order not to introduce water and contaminations to the samples, they were seated on the boat without contacting water. Two heat-treatment curves were applied, (i) elevating from room temperature to 1200 °C holding for 20 h and quenching in air and icy water and (ii) elevating from room temperature to 1250 °C holding for 20 h and quenching in air and icy water. The quenched samples were ground into powders and analyzed via X-ray powder diffraction (XRD, PANalytical X'Pert Pro Powder, Almelo, Netherlands) and software HighScore Plus 4.1 for the identification of the phase assemblages.

4. Results and discussion

4.1. Phase identification and quantification

The quenched samples in the equilibration experiments batch (a) were analyzed employing SEM/EDS and EPMA. EDS owns a weak capability to accurately detect the oxygen content, therefore, EPMA was used to acquire more accurate results. No concentration gradient exists in all the phases of each sample. For the samples equilibrated and quenched at temperatures from 1400 °C to 1620 °C, two homogeneous phases were detected which are molten

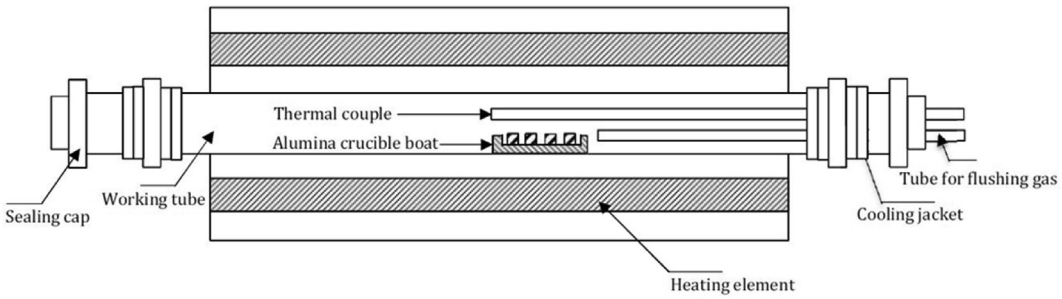

Fig. 3. Schematic picture of the furnace arrangement for equilibration experiment (b).

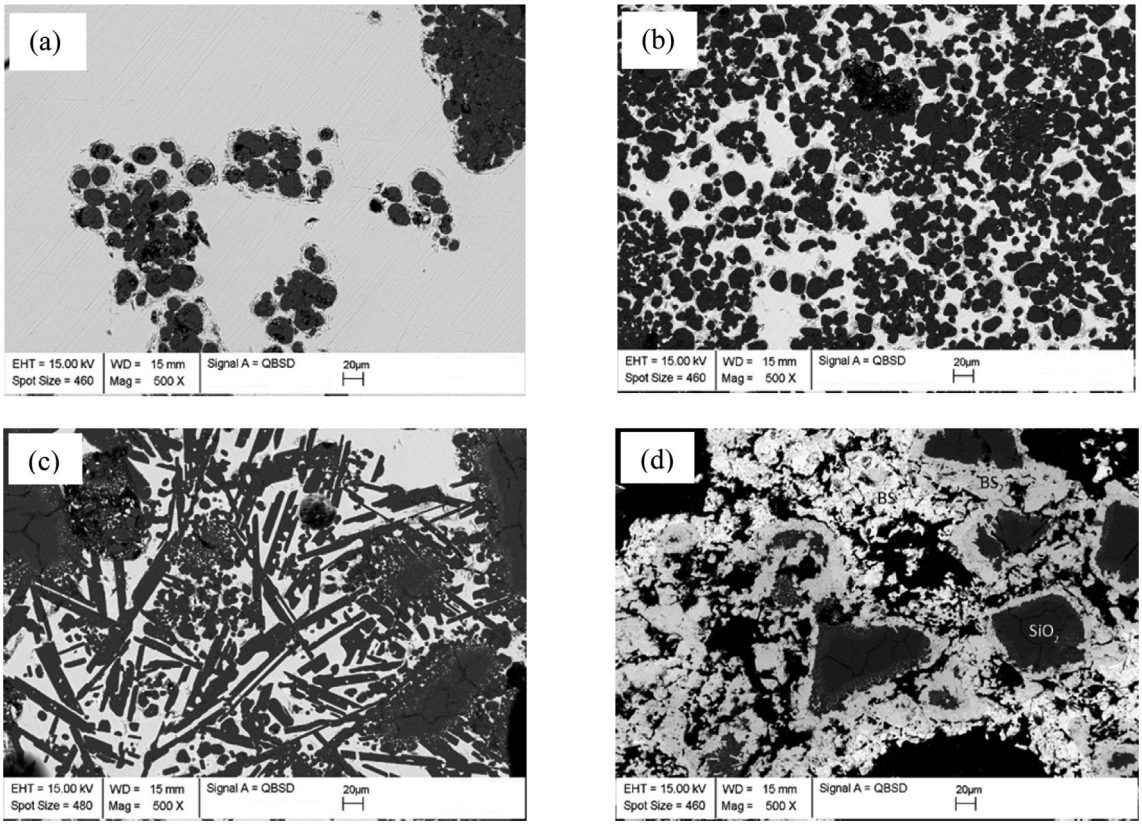

Fig. 4. Back-scattered electron micro-images of samples quenched at (a) 1640 °C, (b) 1500 °C, (c) 1400 °C and (d) 1350 °C. For (a), (b) and (c), dark crystals are SiO_2 and non-crystalline glassy phase is molten phase. For (d), lightest density phase (dark phase) is SiO_2 (phase 1), intermediate density phase is BS_2 (phase 2, wrapping around the SiO_2) and Ba-rich high density phase is BS (phase 3).

phase and SiO_2; and for the temperature at 1350 °C, three distinctive phases were found as BS, BS_2 and SiO_2. The raw data acquired by EPMA are provided in Table 2 with the weight percentage of each element. The total amount of each analysis is 100% ± 3% which demonstrates the success of quenching and guarantees the accuracy of the following calculations.

The normalized EPMA results together with EDS results are presented in Table 3. The individual standard deviations of the EPMA results were calculated and included in the table. It can be observed that the measurements by the two techniques agree well and complete homogeneity of molten phase was achieved in the equilibration and quenching. For the temperatures studied in the present work, the solubility of BaO into SiO_2 as depicted in the Table 3 is small and negligible (lower than 0.2 mol% SiO_2). This corresponds with the phase diagram experimentally constructed and thermodynamically calculated by the authors [11,15,19–21] that no solubility of BaO in SiO_2 is presented.

The phase assemblages identified by XRD for the experiment batch (b) are listed in Table 4. Since the XRD patterns of the samples quenched at 1200 °C and 1250 °C are similar, only the pattern at 1250 °C in this batch are presented in Fig. 5. The results are consistent for the two temperatures studied, 1200 °C and 1250 °C. A minority of BS phase was detected in the samples 4# and 5#. In the view of thermodynamics, phase BS requires more energy to

Table 2
Summary of primary data of the quenched samples in experiment batch (a) analyzed using EPMA.

Temperature	Molten phase (wt.%)				SiO_2 (wt.%)			
	O	Ba	Si	Total	O	Ba	Si	Total
1640 °C	38.13	24.87 ± 0.33	34.74 ± 0.18	97.74	50.82	0.11 ± 0.04	47.40 ± 0.14	98.33
1620 °C	40.53	24.53 ± 0.38	34.03 ± 0.27	99.09	52.27	0.10 ± 0.1	47.44 ± 0.57	99.81
1600 °C	33.94	35.03 ± 0.37	30.04 ± 0.31	99.01	52.08	0.15 ± 0.08	47.38 ± 0.12	99.71
1550 °C	33.75	38.03 ± 0.11	27.61 ± 0.1	99.39	52.14	0.17 ± 0.08	46.27 ± 0.39	98.58
1500 °C	34.17	39.06 ± 0.14	26.26 ± 0.14	99.49	52.20	0.18 ± 0.07	47.04 ± 0.11	99.42
1450 °C	32.84	41.92 ± 0.09	25.14 ± 0.09	99.9	52.52	0.18 ± 0.04	47.12 ± 0.15	99.82
1430 °C	32.90	41.50 ± 0.18	24.99 ± 0.21	99.39	52.76	0.22 ± 0.14	46.25 ± 0.63	99.23
1400 °C	32.06	42.63 ± 0.19	24.75 ± 0.1	99.44	52.41	0.22 ± 0.05	46.69 ± 0.17	99.32
1350 °C	BS_2 (wt.%)				SiO_2 (wt.%)			
	30.14	49.30 ± 0.34	20.06 ± 0.29	100.04	52.95	0.17 ± 0.03	46.38 ± 0.11	99.5
	BS (wt.%)							
	23.46	62.74 ± 0.5	13.21 ± 0.23	99.41				

Table 3
Comparison of the phase composition of the molten phase and the primary crystals analyzed by EPMA and EDS.

Temperature	Phase	EPMA (mol%)			EDS (mol%)	
		SiO_2	BaO	Standard deviation (σ)	SiO_2	BaO
1640 °C	Molten phase	86.55	13.44	0.26	87.7	12.3
	SiO_2	99.95	0.05	0.02	99.8	0.2
1620 °C	Molten phase	86.99	13.01	0.27	87.5	12.5
	SiO_2	99.93	0.07	0.04	99.9	0.1
1600 °C	Molten phase	79.65	20.35	0.2	81.6	18.4
	SiO_2	99.96	0.04	0.01	99.8	0.2
1550 °C	Molten phase	77.40	22.60	0.1	78.2	21.8
	SiO_2	99.93	0.07	0.03	99.8	0.2
1500 °C	Molten phase	76.60	23.40	0.09	77.6	22.4
	SiO_2	99.92	0.08	0.03	99.8	0.2
1450 °C	Molten phase	74.35	25.65	0.1	75.7	24.3
	SiO_2	99.92	0.08	0.02	99.9	0.1
1430 °C	Molten phase	74.53	25.47	0.15	75.1	24.9
	SiO_2	99.90	0.10	0.06	99.8	0.2
1400 °C	Molten phase	73.57	26.43	0.08	73.9	26.1
	SiO_2	99.90	0.10	0.03	99.8	0.2
1350 °C	BS_2	67.36	32.64	0.28	66.5	33.5
	BS	51.71	48.29	0.66	51.5	48.5
	SiO_2	99.92	0.08	0.01	99.0	1

Table 4
Summary of X-ray analysis of samples (1–5#) in the equilibration experiment (b).

Equilibration condition	Samples (molar ratio of BaO: SiO_2)				
	1# (0.7:0.3)	2# (0.6:0.4)	3# (0.45:0.55)	4# (0.39:0.61)	5# (0.35:0.65)
Argon (99%) + H_2 (1%) 1200 °C, 42 h → air and icy water quenching	$B_3S + B_2S$	$B_2S + BS$	$B_2S_3 + BS$	$B_2S_3 + B_5S_8 + BS$ (trace)	$B_5S_8 + BS_2 + BS$ and B_2S_3 (trace)
Argon (99%) + H_2 (1%) 1250 °C, 42 h → air and icy water quenching	$B_3S + B_2S$	$B_2S + BS$	$B_2S_3 + BS$	$B_2S_3 + B_5S_8 + BS$ (trace)	$B_5S_8 + BS_2 + BS$ and B_2S_3 (trace)

decompose compared with B_5S_8 and BS_2 because it has larger Gibbs energy than the other two phases. The evidence to prove this explanation can be obtained from the calculated molar Gibbs energy of all the stoichiometric compounds of the system in Fig. 6. The molar Gibbs energies were obtained from the MTOX oxide database [10].

4.2. Microstructural morphology

The typical back-scattered electron micrographs are shown in Fig. 4. Since the phases in different samples quenched at 1400 °C–1640 °C possess similar morphology, the graphs in Fig. 4 are the representative ones. The co-existence of crystals and non-crystalline molten phase can be observed at and above 1400 °C. As temperature decreases from 1640 °C to 1400 °C, the amount of molten phase is depleting accordingly with more crystals forming. For the sample quenched at 1350 °C (d) in Fig. 4, no liquid phase was identified but three phases with different densities can be found. On the basis of the EDS and EPMA results, they are SiO_2 (dark phase), BS_2 (wrapping around SiO_2) and BS (Ba-rich high density

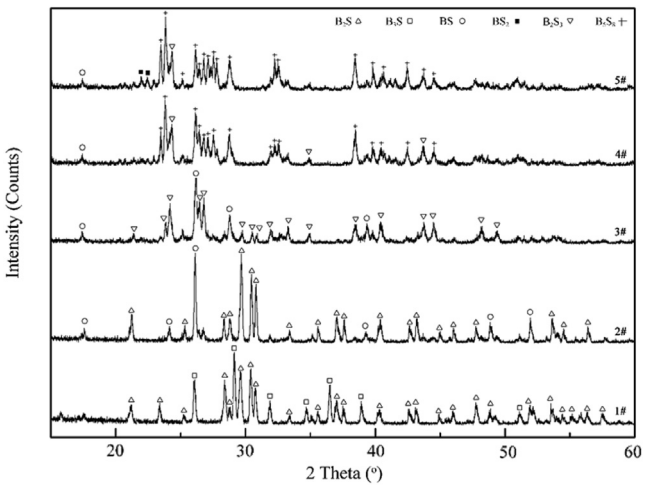

Fig. 5. X-ray diffraction patterns of samples in the experiment batch (b).

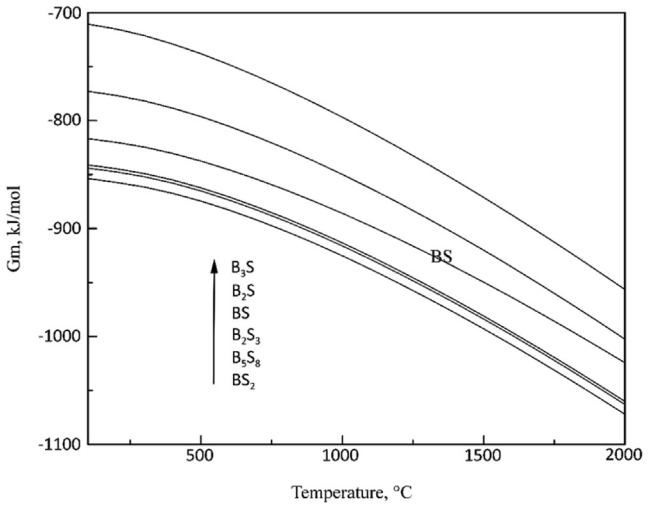

Fig. 6. Calculated molar Gibbs energies of the stoichiometric compounds in the BaO–SiO_2 system based on MTOX oxide database [10].

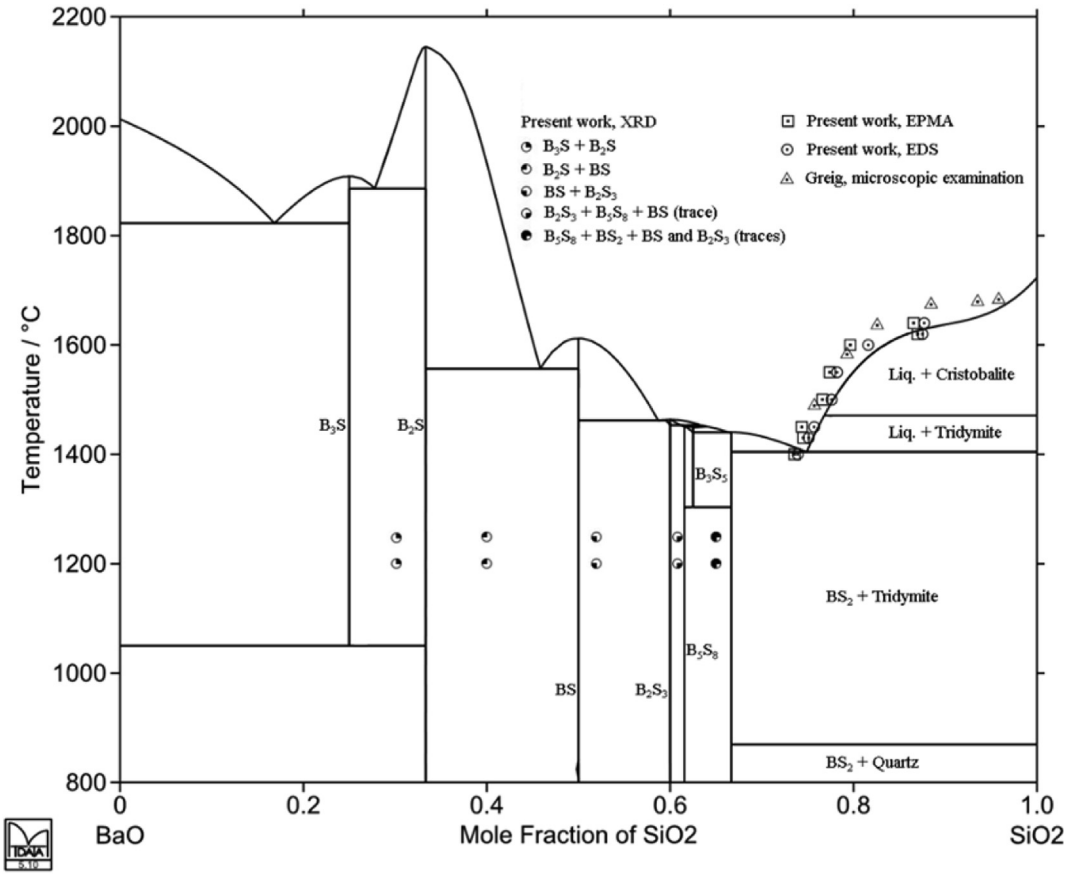

Fig. 7. Calculated phase diagram of the BaO–SiO_2 system, compared with the present experiments and literature data.

phase). A study made by Ref. [23] concerning the reaction sequence between barium carbonate and aluminum oxide presents a possible mechanism that barium oxide firstly reacts with aluminum oxide to form BA ($BaAl_2O_4$) as an intermediate phase, and then BA reacts excess aluminum oxide to give BA_6 ($BaAl_{12}O_{19}$) which is the compound containing highest amount of aluminum oxide in the BaO–Al_2O_3 system. This study can be used as an analogy to interpret the co-existence of three phases in the sample equilibrated and quenched at 1350 °C in the present work. The firstly formed BS phase reacted with excess SiO_2 to achieve BS_2. And a trace amount of BS was remained due to the highest molar Gibbs energy itself as discussed in the Section 4.2. Further investigation is required to verify this possible mechanism applied in BaO–SiO_2 binary system.

4.3. Thermodynamic calculations

The calculation of the BaO–SiO_2 system was carried out with MTDATA, version 5.10 []. The assessed thermodynamic parameters in MTOX database version 8.1 [10] were employed for the description of molten phase, BS, B_2S, B_3S_5, B_5S_8, B_2S_3, B_3S and BS_2.

In Fig. 7, the present experimental points and the available literature data are compared with the calculated phase diagram of the BaO–SiO_2 system based on the MTOX oxide database [10]. The calculation can well reproduce the present experimental data for liquidus. According to the analyzed results for the sample quenched at 1350 °C, no molten phase can be found and at 1400 °C liquid coexisting with SiO_2 can clearly be observed. Consequently, the estimated temperature of the eutectic reaction, liquid → BS_2 + tridymite, is between 1350 °C and 1400 °C, which is a little lower than the calculated eutectic reaction temperature (1405 °C) in Fig. 7. More experimental equilibria data and a new thermodynamic assessment are needed in the future to confirm the exact eutectic temperature of this reaction.

5. Conclusions

The liquidus in the SiO_2-rich region of the BaO–SiO_2 binary system was experimentally constructed based on the EPMA and SEM/EDS results by analyzing the samples quenched at temperatures from 1400 °C to 1640 °C. Coexistence of a homogeneous molten phase and SiO_2 was observed and quantified. The solubility of BaO in SiO_2 is smaller than 0.2 mol% SiO_2 and negligible. The stabilities of B_3S, B_2S, BS, B_2S_3 and B_5S_8 were confirmed at 1200 °C and 1250 °C. The temperature of the eutectic reaction, liquid → BS_2 + tridymite, was estimated to be between 1350 °C and 1400 °C. Phase diagram of the BaO–SiO_2 system and molar Gibbs energy of B_3S, B_2S, BS, B_2S_3 and B_5S_8 were calculated on the basis of MTOX oxide database [10] using the software MTDATA [22]. The calculated liquidus in the SiO_2-rich side agrees well with the measured liquidus in the present work. In the future studies, particular attention in respect of thermodynamic assessment and experimental measurements should be paid to the solid-state decomposition temperatures of the phase B_3S in the BaO-rich corner and the phase B_3S_5 existing between B_5S_8 and BS_2.

Acknowledgment

This research was financially supported by Association of Finnish Steel and Metal Producers, Tekes and System Integrated

Metal Processes (SIMP) program by FIMECC. The assistance of Dmitry Sukhomlinov, Joseph Hamuyuni and Petteri Halli in the experimental part is greatly appreciated.

References

[1] A. Young, G. Hilmas, S.C. Zhang, R.W. Schwartz, J. Am. Ceram. Soc. 90 (2007) 1504–1510.
[2] T. Wang, L. Jin, L.L. Shu, Q.Y. Hu, X.Y. Wei, J. Alloys Compd. 617 (2014) 399–403.
[3] S. Chen, D.G. Zhu, J. Alloys Compd. 536 (2012) 73–79.
[4] S. Chen, S.R. Zhang, X.H. Zhou, Z. Wen, J. Alloys Compd. 509 (2011) 4848–4853.
[5] C. Acuña, A. Yazawa, Trans. ISIJ. 28 (1987) 498–506.
[6] I.V. Koj, P.A. Taskinen, Lilius, Met. Trans 16B (1985) 171.
[7] J. Chipman, Metal Prog. 62 (1952) 97–107.
[8] J. Chipman, L.C. Chang, AIME Trans. 185 (1949) 191–197.
[9] G.S. Powley, T.P. Floridis, Met. Trans. 1 (1970) 311–313.
[10] MTOX oxide database, Release Notes for Version 8.1 of Mtox Database, National Physical Laboratory, Teddington, UK, 2015.
[11] J.W. Greig, Am. J. Sci. 13 (1927) 1–44.
[12] J.B. Ferguson, H.E. Merwin, Am. J. Sci. 46 (1918) 417–426.
[13] F.C. Kracek, J. Am. Chem. Soc. 52 (1930) 1436–1442.
[14] Y.I. Ol'shanskij, PP, Dokl. Akad. Nauk SSSR 76 (1951) 93–96.
[15] P. Eskola, Am. Jour. Sci. 4 (1922) pp.343–375.
[16] E.M. Levin, G.M. Ugrinic, J. Res. Nat. Stand. 51 (1953) pp.37–56.
[17] R.S. Roth, E.M. Levin, J. Res. Nat. Stand. 62 (1959) pp.193–200.
[18] R.M. Douglass, Am. Mineral. 43 (1958) 517.
[19] A. Shukla, Development of a Critically Evaluated Thermodynamic Database for the Systems Containing Alkaline-Earth Oxides, Ecole Polytechnique de Montreal, Canada, 1–321.
[20] A.R. Serrano, A.C. Ramirez, B. Zeifert, M.H. Lopez, A.H. Ramirez, Glass Phys. Chem. 36 (2010) 171–178.
[21] E. Boulay, J. Nakano, S. Turner, H. Idrissi, D. Schryvers, S. Godet, CALPHAD 47 (2014) 68–82.
[22] R.H. Davies, A.T. Dinsdale, J.A. Gisby, J.A.J. Robinson, S.M. Martin, CALPHAD 26 (2002) 229–271.
[23] J. Beretka, T. Brown, Aust. J. Chem. 26 (1973) 2527–2531.